Microscopy and Microanalysis (2022), **28**, 1679–1686
doi:10.1017/S1431927622000708

Microscopy AND Microanalysis

Original Article

Minimizing Motion Artifacts in Intravital Microscopy Using the Sedative Effect of Dexmedetomidine

Youngkyu Kim[1,a], Minju Cho[1,a], Bjorn Paulson[1], Sung-Hoon Kim[2]* and Jun Ki Kim[1,3]*

[1]Biomedical Engineering Research Center, Asan Medical Center, Seoul 05505, Republic of Korea; [2]Department of Anesthesiology and Pain Medicine, Asan Medical Center, University of Ulsan College of Medicine, 88, Olympic-ro 43-Gil, Songpa-gu, Seoul 05505, Republic of Korea and [3]Department of Convergence Medicine, University of Ulsan, College of Medicine, 88, Olympic-ro 43-Gil, Seoul 05505, Republic of Korea

Abstract

Among intravital imaging instruments, the intravital two-photon fluorescence excitation microscope has the advantage of enabling real-time 3D fluorescence imaging deep into cells and tissues, with reduced photobleaching and photodamage compared with conventional intravital confocal microscopes. However, excessive motion of organs due to involuntary movement such as breathing may result in out-of-focus images and severe fluorescence intensity fluctuations, which hinder meaningful imaging and analysis. The clinically approved alpha-2 adrenergic receptor agonist dexmedetomidine was administered to mice during two-photon fluorescence intravital imaging to alleviate this problem. As dexmedetomidine blocks the release of the neurotransmitter norepinephrine, pain is suppressed, blood pressure is reduced, and a sedation effect is observed. By tracking the quality of focus and stability of detected fluorescence in two-photon fluorescence images of fluorescein isothiocyanate-sensitized liver vasculature *in vivo*, we demonstrated that intravascular dexmedetomidine can reduce fluorescence fluctuations caused by respiration on a timescale of minutes in mice, improving image quality and resolution. The results indicate that short-term dexmedetomidine treatment is suitable for reducing involuntary motion in preclinical intravital imaging studies. This method may be applicable to other animal models.

Key words: alpha-2 adrenergic receptor agonist, dexmedetomidine, hypotension, imaging resolution improvement, intravital imaging

(Received 23 February 2022; revised 15 April 2022; accepted 2 May 2022)

Introduction

Since the invention of the microscope, intravital imaging has enabled the nondestructive visualization of dynamic biological processes in the cells and tissues that make up living organisms (Coste et al., 2020). Intravital microscopy techniques have been employed to observe a variety of tissue–cell interactions showing cellular and tissue dynamics (Pittet & Weissleder, 2011; Choo et al., 2020; Soulet et al., 2020). Because intravital imaging tools provide real-time visualizations via nondestructive methods, they can be widely used for research and diagnosis.

Two-photon-excited fluorescence microscopy is a particularly useful form of intravital microscopy. Pioneered by Denk and Webb in 1990 using subpicosecond pulsed lasers, the mechanism of highly localized fluorescence through nonlinear excitation processes allows highly localized fluorescence (Denk et al., 1990). It also permits the use of infrared wavelengths that penetrate deep into tissues (Helmchen & Denk, 2005, 2006) and reduce photobleaching and photodamage compared with the use of white light in confocal microscopy (Koenig et al., 1996). Two-photon microscopes enable 3D-resolved fluorescence imaging of highly scattering live cells deep inside thick tissues, as well as the long-term imaging of photosensitive biological specimens with reduced phototoxicity (Denk et al., 1990; Zipfel et al., 2003; Noh et al., 2021). Preclinical observations enabled by the two-photon microscope have included the interaction integrity of glioblastoma cells with the tumor microenvironment (Pichol-Thievend et al., 2021), the cellular interactions which contribute to biliary membrane integrity (Vats et al., 2021), and the fast spatiotemporal cellular dynamics within neural networks (Laffray et al., 2011). Two-photon microscopes have been used to discriminate tumor-adjacent cancer cells tagged with fluorescent enzymes (Noh et al., 2021).

However, even when the mice are under anesthesia, severe tissue movement occurs because of respiration and (to a lesser extent) pulmonary circulation. Tissue movement may result in out-of-focus images, may impede meaningful imaging owing to the severe fluorescence intensity variations, and could add motion artifacts to images, compromising image sharpness and resolution (Lee et al., 2012; Vinegoni et al., 2014). Therefore, motion compensation and tissue stabilization are important challenges in intravital imaging (Matsuura et al., 2018) for which many techniques have been devised. While early attempts to compensate for physiological motion took advantage of stroboscopy (DeFily, 1997), more recently frame-by-frame motion compensation algorithms have been developed for use during image acquisition. Unfortunately, real-time compensation is limited if there is

[a]These authors contributed equally to this work.

***Corresponding authors:** Jun Ki Kim, E-mail: kim@amc.seoul.kr, Sung-Hoon Kim, E-mail: shkimans@gmail.com

Cite this article: Kim Y, Cho M, Paulson B, Kim S-H, Kim JK (2022) Minimizing Motion Artifacts in Intravital Microscopy Using the Sedative Effect of Dexmedetomidine. *Microsc Microanal* **28**, 1679–1686. doi:10.1017/S1431927622000708

distortion in the frame (Pnevmatikakis & Giovannucci, 2017). In addition, motion correction may need to be performed several times for areas with high motion (Dold et al., 2006). Therefore, for performing intravital imaging, methods including the use of fixed adhesive rings and imaging windows have been proposed. However, these methods may cause toxic reactions owing to the adhesive chemicals involved, or unintended adhesions to the organ (Woodward et al., 1965). In addition, surgical methods must be weighed against the potential for unexpected side effects (Park et al., 2020), and the existing surgical methods to reduce movement and physically immobilize external organs cannot guarantee stable high-resolution images. In particular, peristalsis in the intestine causes high-amplitude movements that are not compensated for by physical restraint alone. Papaverine, an opioid alkaloid that is mainly used in the treatment of vascular spasms owing to its vasodilatory effect (Kassell et al., 1992; Girard et al., 2004), has been used to treat spasms of the gastrointestinal tract (Anderson & Fredericks, 1977). Instead of applying physical control or using an algorithm, we propose a minimally invasive method that lowers blood pressure and heart rate with a sedative effect.

Dexmedetomidine (DEX; (S)-4-[1-(2,3-dimethylphenyl) ethyl]-3H-imidazoleacts]) is an α_2-adrenergic receptor agonist and is clinically used as an analgesic, sedative, and anxiolytic agent, with known protective effects against fear-related and anxiety-like behaviors (Jang et al., 2019) and no noted withdrawal symptoms (Venn et al., 1999; Gertler et al., 2001; Yu, 2012). The presynaptic activation of α_2 adrenergic receptors inhibits the release of norepinephrine, which relieves pain. Because the postsynaptic activation of α_2 adrenergic receptors suppresses sympathetic nerve activity and reduces heart rate, the use of dexmedetomidine has a sedative effect as well as an analgesic effect (Nelson et al., 2003; Cai et al., 2014). In particular, DEX is a highly selective and potent α_2 adrenergic agonist, and α_2 receptors are involved in the regulation of hemodynamic response (Philipp et al., 2002). For this reason, oral administration of α_2 receptor agonists predominates in hypotensive action, and intravenous administration causes arterial pressure to drop below normal. This causes cardiovascular stability issues during sedation with DEX and significant rate-pressure product reduction has been shown (Venn et al., 2000). On comparing its sedative effect with that of propofol in clinical trials, DEX administration was found to significantly lower the heart rate (Nelson et al., 2003; Hughes et al., 2021). With the use of DEX, blood pressure and heart rate may be controlled, resulting in clearer and more accurate imaging as tissue motion artifacts caused by the respiratory movement of mice during intravital imaging are minimized. Moreover, DEX is unlikely to have significant side effects on mice if used during intravital imaging, because it shows nonneurotoxic properties even when high doses are injected during rat surgery (Elbaradie et al., 2004).

In this study, blood flow through the liver tissue of mice was imaged using a two-photon intravital microscope and fluorescein isothiocyanate (FITC), a vascular fluorescence contrast agent (Ihler et al., 2015). A variety of doses of dexmedetomidine were injected, and the effect of the resultant sedation upon fluorescent vascular imaging over time was evaluated via two-photon excitation microscopy. We quantitatively evaluated whether high-resolution imaging could be obtained from sedated mice by evaluating the focus of fluorescent images, the consistency of fluorescence, and the motion of red blood cells over time. It was found that at the doses studied, dexmedetomidine has a measurable stabilizing effect on imaging, which was the highest and most consistent at 7 min after injection. This experiment provides indications for the optimal dose and duration of DEX for *in vivo* imaging, along with suggestions for future uses.

Materials and Methods

Animal Model

C57BL/6 mice were purchased from OrientBio (Seong-nam, Korea). Eight-week-old male mice weighing an average of 20 g each ($N = 4$) were used for the experiment. The experiment was conducted under the guidance and regulations of the Institutional Animal Care and Use Committee (IACUC) of Asan Medical Center (protocol # 2021-12-276). The mice were housed in ventilated cages at room temperature; food and water were freely accessible, and the lighting followed a normal day/night cycle.

Anesthesia

The mice were anesthetized using an intraperitoneal 3:2 solution of zolazepam-tiletamine (Zoletil 50, Virback, Carros cedex, France) and xylazine (Rompun, Elanco, Seoul, Republic of Korea). A total of 2 mL anesthetic solution was prepared by adding 120 μL Zoletil and 80 μL xylazine to 1,800 μL of phosphate-buffered saline (Gibco DPBS, Thermo-Fischer Scientific Korea, Seoul, Republic of Korea). Protocols called for 10-μL anesthetic solution per gram of body weight. As the average weight of the mice was 20 g, 200 μL of the solution was used to anesthetize each mouse.

Dexmedetomidine Treatment

Dexmedetomidine (Dexmedine in 200 mcg, Hana Pharm Co. Ltd., Seoul, Republic of Korea) was obtained in syringes containing a single human dose each and partitioned among the animals, with 0.25 μg, 0.75 μg, 1.0 μg, or 1.5 μg administered to each mouse. Dexmedetomidine was injected into the lateral tail vein using a syringe pump (Fusion 200, Chemyx Inc., Stafford, TX, USA).

Vascular Fluorescence

FITC-dextran (FITC, avg. mol. wt. 2.0 MDa, Sigma-Aldrich, Seoul, Republic of Korea) was prepared on the day of imaging at 50 mg/mL in DPBS. Each mouse was injected with 50 μL of solution in the orbital venous sinus prior to the experiment.

Intravital Imaging Setup

A two-photon microscope (IVIM Technology, Daejeon, Korea) was used with an animal stage chamber, a syringe pump, and a PC connected for real-time imaging, as shown schematically in Figure 1. The microscope included a 25× water immersion objective (Apo LWD 25x/1.10W, Nikon), and the animal stage chamber had sliding doors and ports which allowed the heating pad controller and syringe pump tubes to enter the microscope enclosure while reducing the background signal. After anesthetizing a mouse with Zoletil and Rompun, FITC was injected into the orbital vein. Then, a transverse incision was made in the middle of the abdomen to expose the liver. The liver was placed on a

https://doi.org/10.1017/S1431927622000708 Published online by Cambridge University Press

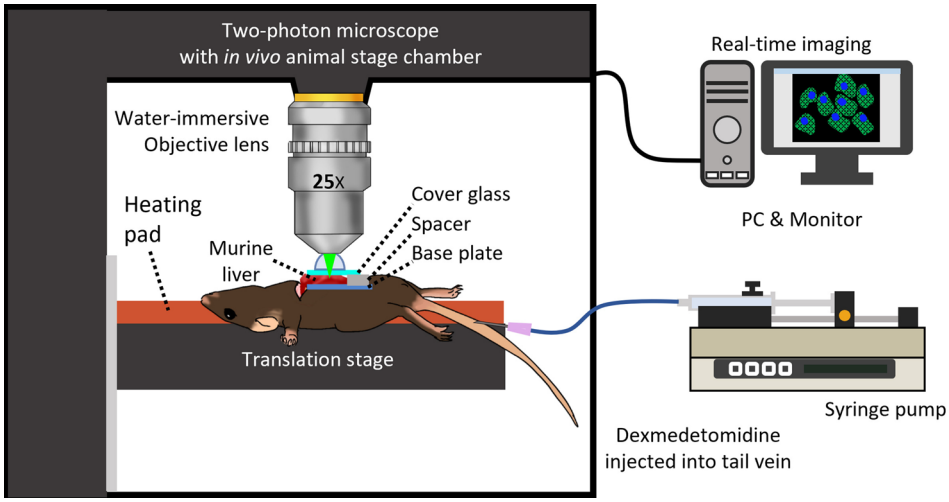

Fig. 1. Schematic of the experiment: an enclosed two-photon microscope set up for animal experiments with a syringe pump for intravenous injection of dexmedetomidine (DEX).

base plate. To maintain body temperature, the mouse was placed on a translation stage with a heating pad set to 36°C. A cover glass was placed on the exposed liver to flatten the surface, and a drop of water was added for water immersion. Once the imaging environment was prepared, the syringe was inserted into the caudal vein of the mouse, and DEX was injected at a constant speed using the syringe pump, while the effect of DEX was imaged in real-time.

Image Acquisition

An IVM-MS laser-scanning intravital two-photon microscope (IVIM Technology, Daejeon, South Korea) was used for image acquisition. It incorporates a femtosecond pulsed laser (wavelength 920 nm and pulse duration less than 140 fs) and has four detector channels (second harmonic, GFP, RFP, far red). FITC-dextran was imaged on the GFP channel (520 ± 12.5 nm). Images were acquired at a resolution of 1,024 pixels × 1,024 pixels and 15 fps for 10 s.

Image Analysis

After acquiring image data, we used MATLAB® (MathWorks, MA, USA) for image analysis. The MATLAB Image Processing Toolbox provides functions for calculating the intensity of each pixel. A total of 150 frames, 1,024 pixels × 1,024 pixels each, were loaded and the difference in average absolute intensity was calculated between adjacent image frames. The average absolute intensity differences were calculated by taking the difference in intensities between pixels at the same coordinate position in each of the two image frames, and then averaging their absolute values, as follows:

$$\frac{1}{n}\sum_{i,j} |\, I_1(i,j) - I_2(i,j)|,$$

where $I_1(i,j)$ and $I_2(i,j)$ are the pixel intensities at the (i,j)-th pixel position, n is the total number of pixels in one frame, and the sum is taken over all pixels in the frame.

Results

Green fluorescence was expressed in the blood vessels of the mouse liver by administering FITC and was imaged using video-rate two-photon microscopy, as shown in Figure 2. These images captured the fluorescence intensity from the outer surface of the mouse liver before DEX injection and at the same location after the mice were injected with 1.5 μg DEX. Observations were made at 3 min, 7 min, and 11 min postinjection. For each observation, images were captured for 10 s at a rate of 15 images per second, resulting in a video with 0.067 s between adjacent frames. Fluctuations in the fluorescence intensity were observed in the liver tissue on comparing the difference in the fluorescence between frames, which were nominally focused to the same depth. On comparing the difference in the fluorescence of the images before DEX injection and 7 min after DEX injection, we observed that there was a change in the fluorescence area due to improved focus as the image was stabilized. Stabilization continued up to 11 min after DEX injection.

While the images in the first two columns of Figure 2 show snapshots of the fluorescent-labeled liver surface vascularization at different points in time (0.2 s apart) after DEX dosing, the color images in the third column show the difference when these images are overlapped. With the two images overlapped, the color mismatches are clear, and within 7 min after DEX injection, a clear decrease in movement was observed. The fourth column is the average image during the 10-s imaging time. Blurry images before DEX injection indicate mismatches in focus or lateral movement, and it can be seen that these were reduced after injecting DEX. This is clearly confirmed in the fifth column of Figure 2, where an enlarged subframe is shown. While the averaged image before DEX injection was blurry, indicating significant movement, the image quality improved after DEX injection. The vessel image appears blurry until 3 min postinjection; however, the image quality improved after 7 min postinjection.

The intensity of the fluorescence region was also measured and compared in this dataset. Figure 3 shows graphs of the quantity calculated by averaging the absolute value of the difference in intensity between corresponding pixels in sequential frames (the L1 norm between sequential frames) over the full pixel domain. As the fluorescent tissue images are arrays of 8-bit integers, the

https://doi.org/10.1017/S1431927622000708 Published online by Cambridge University Press

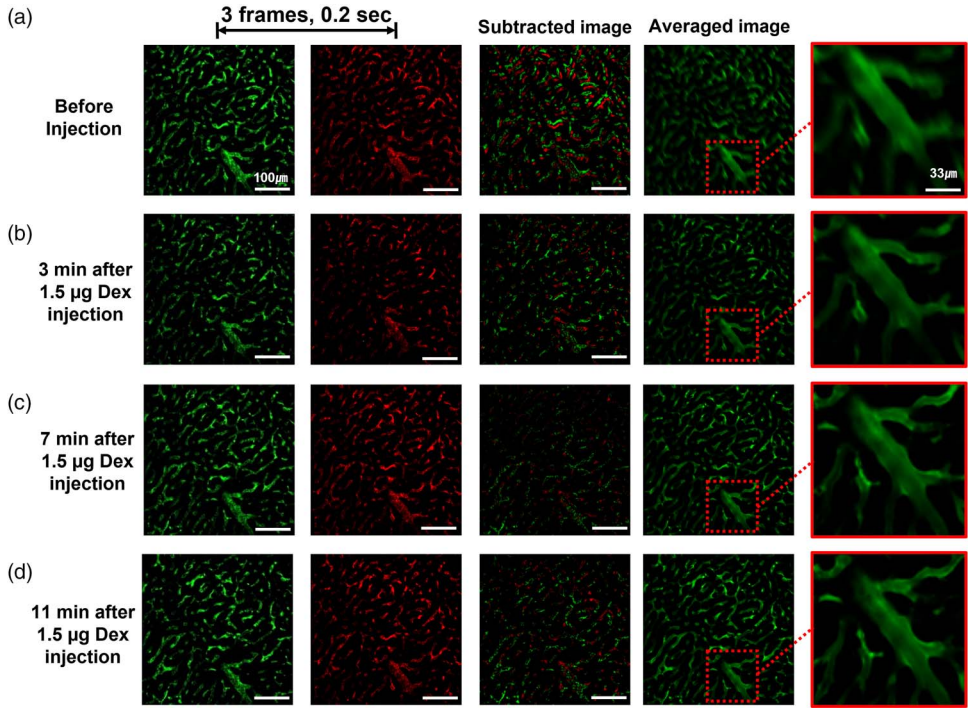

Fig. 2. Two-photon micrographs showing the stabilization effect and resolution-increasing effect of DEX on fluorescent microscopy of the mouse liver. (**a**) Microscopy of the liver before DEX injection (Supplementary Movie 1), (**b**) 3 min after 1.5 μg DEX injection (Supplementary Movie 2), (**c**) 7 min after injection (Supplementary Movie 3), and (**d**) 11 min after injection (Supplementary Movie 4).

L1 average falls in the range of 0 to 255, and the intensity of each pixel changes over time following the movement of the tissue. The graphs for each DEX dosage were normalized together.

On comparing the intensities between pixels on the same location of each frame (as shown in Fig. 3, and summarized graphically in Fig. 4), the largest amplitudes were observed before DEX was injected. The difference in the intensity of fluorescence was high whenever the mouse breathed, that is, periodically with a period of about 2 Hz. In Figure 3a, which shows the observed fluorescence fluctuations for the mouse injected with 0.25 μg DEX, both the mean values and the maximum amplitudes of every plot are reduced compared with those of the preinjection plot. The average pixel intensity difference was 0.4 before 0.25 μg of DEX was injected. However, 3 min after DEX injection, the amplitude decreased and the average pixel intensity difference reached its lowest point, with an average of about 0.15. After 7 min, the average pixel intensity difference increased minimally, recording an average value of 0.2, and this value was maintained until 11 min after injection as shown in Figure 4. In the mouse injected with 0.75 μg of DEX, the average pixel intensity difference before DEX injection was between 0.4 and 0.6, and by 3 min after DEX injection, the average value dropped to 0.3. After 7 min, the average value increased and remained stable until 11 min (Fig. 4). In the case of the mouse injected with 1.0 μg DEX, the average value of the pixel difference amplitude before DEX injection was slightly less than 0.6 but hit its minimum value 3 min after DEX injection. It increased again after about 7 min and remained constant until 11 min thereafter. In the mouse treated with 1.50 μg DEX, the average difference decreased significantly after DEX injection, and the amplitude difference lowered noticeably. This phenomenon was maintained until 11 min after DEX injection.

The flow velocity of the blood was captured via microscopy. As shown in Figure 5, the point marked with a white box is a blood cell that moves through every frame, and tracking its motion allows the flow of blood to be analyzed. The difference in the distance traveled by the blood cell was compared after 1 min, 3 min, and 7 min in the mouse injected with 1.5 μg DEX. As seen in Figure 5, the distance that a blood cell traveled 1 min after DEX delivery over 0.133 s and the distance a similar cell traveled in an equivalent time period 7 min after injection were significantly different; the blood flow peaked 1 min after injection and then reduced, leveling off between 7 and 11 min postinjection.

The rate of blood flow was calculated in μm/s and is plotted in Figure 5d. Before DEX injection, the blood flow was measured to be 100 μm/s. Three minutes after DEX was injected, the rate of blood flow increased to 120 μm/s, after which it decreased sharply before leveling off around 80 to 90 μm/s between 7 and 11 min after DEX injection.

Discussion

By comparing intravital two-photon fluorescence excitation microscopy measurements before and after the injection of DEX, we observed a phenomenon in which breathing and cardiac movement were stabilized during intravital imaging, resulting in improved fluorescence images and videos. As seen in Figure 2, consistency of the imaging region (and the ability to perform long-exposure images) was improved by 5 to 7 min after treatment with DEX, and higher dosages had improved effects. The fluorescence intensity was found to vary less under DEX treatment, and the blood flow rate in the liver surface was found to increase transiently. By reducing the movement of cells and tissues due to an animal's respiration and pulse, we enabled high-quality *in vivo* imaging.

https://doi.org/10.1017/S1431927622000708 Published online by Cambridge University Press

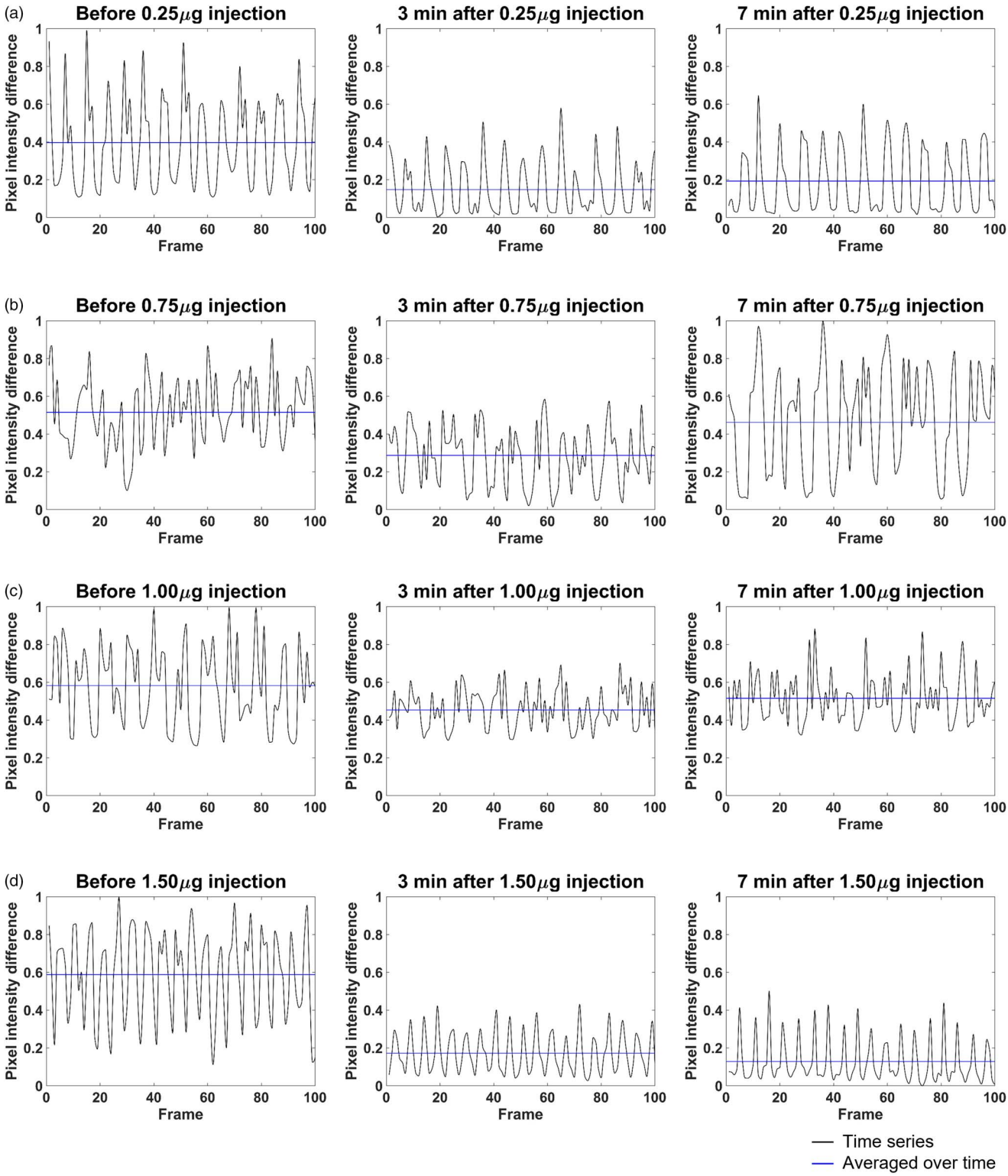

Fig. 3. The normalized L1 norm between sequential frames over time, in the case of (**a**) 0.25 μg DEX injection, (**b**) 0.75 μg DEX injection, (**c**) 1.00 μg DEX injection, and (**d**) 1.50 μg DEX injection.

It is worthwhile to caution against the overinterpretation of results. The design of this study was exploratory, and the sample size ($N = 4$) was small, compared with other animal experiments. Due to the small sample size and unavoidable experimental factors such as the impossibility of identically exteriorizing mouse livers, variance in the part of the liver being imaged, and variation in metabolism and drug response between the individual mice, there is expected to be some variation in the results. However, this longitudinal study utilizing intravital imaging techniques removes many sources of bias and makes a spurious finding

https://doi.org/10.1017/S1431927622000708 Published online by Cambridge University Press

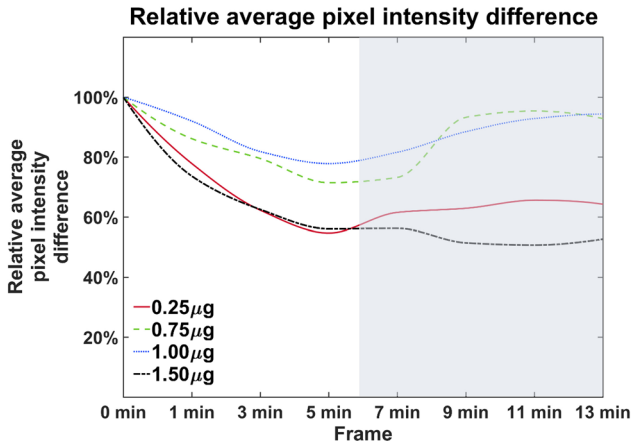

Fig. 4. The relative average pixel intensity difference shows consistency in reduced movement until 7 min post injection.

less likely: the stabilizing effect increases with dosage and follows a consistent time series, which suggests a relationship with the pharmacokinetics and metabolism of DEX in mice. In humans, DEX has been found to distribute rapidly to tissues, with a distribution half-life of about 6 min and a mean elimination half-life of 2–2.5 h (Karol & Maze, 2000). The short timespan associated with DEX uptake in tissues by Karol and Maze matches well with the duration of the sedative effect which was observed in this study, although further studies are required to determine the limitations of DEX for stabilizing preclinical microscopy (i.e., build-up or tolerance development in mice).

There is reason to believe that treatment with DEX will also generalize to other animal models. Dexmedetomidine is also used as a sedative for dogs and is known to result in a decrease in heart rate without significant variance based on body weight, age, or sex. In addition, when a laryngeal examination was performed using dexmedetomidine in dogs, it was noted to be an effective sedative and did not affect arytenoid abduction while preventing jaw movement (Micieli et al., 2017; DeGroot et al., 2020).

Historically, many strategies have been used to overcome the challenge of involuntary movement during intravital microscopic imaging, including but not limited to the use of adhesives, stroboscopy, clamps, pins, stereotactic mounts, and electro-optic motion compensation. Unlike previous strategies, the method proposed here does not require changes to the optical setup, nor does it require careful setup or surgery. Thus, treatment with DEX is a less invasive and "low-tech" method of reducing involuntary movement.

Presently, there is much excitement in the microscopic research community regarding algorithmic methods for image stabilization, driven by the blossoming of deep learning and artificial intelligence for image processing. However, each of these methods comes with associated tradeoffs: real-time sharpening algorithms based on combining data from adjacent frames often reduce the practical frame rate, and the designers of deep learning-based algorithms must remain vigilant for artifacts "hallucinated" by the algorithm. Thus, although there is little doubt that the future of intravital microscopy will make widespread use of algorithmic image stabilization, physical stabilization, and pharmacological stabilization through compounds like dexmedetomidine will likely serve as an initial filter for removing unwanted movement.

While the present study is limited to preclinical animals, dexmedetomidine is suitable for translation to the clinic to reduce physiological motion during next-generation endomicroscopic imaging. As DEX is FDA-approved for clinical use with an indication for sedation of nonintubated patients prior to and/or during surgical and other procedures, and has a well-known risk profile, there is potential for its application in translational imaging. (Shukry & Miller, 2010). While it is commonly used in operating theaters as a sedative, analgesic, and anxiolytic agent, its intraoperative administration also improves postoperative analgesic effects (Afonso & Reis, 2012; Hong et al., 2012; Ding et al., 2015). Recently, DEX has been demonstrated to improve pediatric MRI imaging (Mason et al., 2011). Its incorporation into modern clinical imaging workflows will require no modification to imaging technology and would likely be beneficial for physicians, as it would provide additional stabilization for images captured by next-generation endoscopes, colonoscopes, and laparoscopes

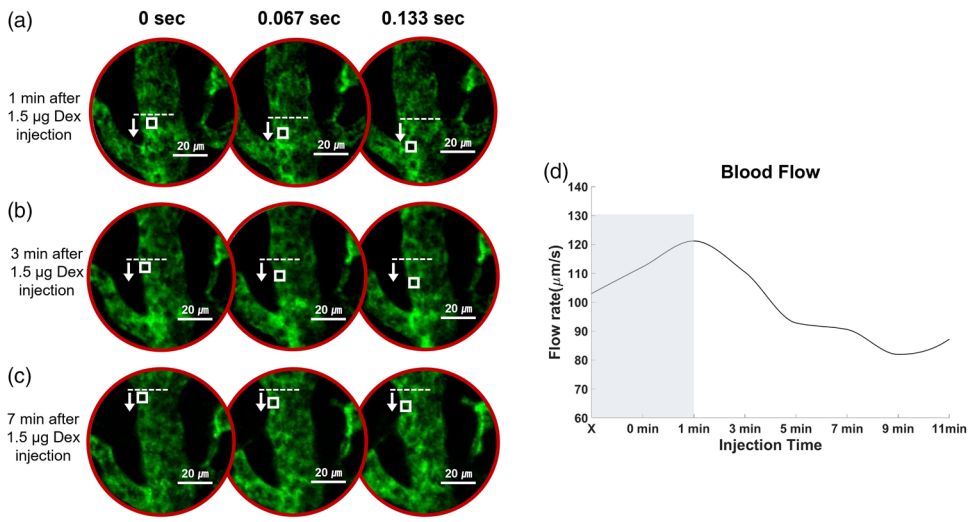

Fig. 5. Tracking cells from intravital measurements enables the determination of the effect of DEX on blood flow. Blood flow (**a**) 1 min following injection of 1.5 μg DEX, (**b**) 3 min after DEX injection, (**c**) 7 min after 1.5 DEX injection, and (**d**) the measured rate of blood flow plotted over time.

https://doi.org/10.1017/S1431927622000708 Published online by Cambridge University Press

equipped with cellular-resolution endomicroscopy technologies (Kim et al., 2012; Belykh et al., 2018; Lesur et al., 2019; Yin et al., 2019; Pilonis et al., 2022). However, in clinical settings, there are other methods for regulating the involuntary movement of patients. Our findings will simplify time-course animal microscopy studies.

When administering DEX for intravital imaging, potential local cellular-level changes in the physiological environment should be considered. Administration of DEX may interfere with the biomarkers that are to be analyzed by intravital imaging by affecting microcirculation or hemodynamics. DEX is a selective a2-adrenoreceptor agonist with sedative and analgesic properties and is almost eight times more specific than clonidine (Giovannitti et al., 2015). Intravenous administration of DEX, however, induces significant hypotension and bradycardia until the central sympatholytic effects diminish (Bloor et al., 1992; Civantos Calzada & Aleixandre de Artiñano, 2001). The hypotensive effect of DEX is dose-dependent. A previous study has shown that heart rate, cardiac output, and norepinephrine concentrations decrease progressively with increasing DEX concentrations, but DEX causes a biphasic change in blood pressure (Ebert et al., 2000). At low concentrations (<1.9 ng/mL), mean arterial pressure decreases, followed by increasing mean arterial pressures observed with increasing DEX concentrations (Ebert et al., 2000). It is thought that activation of peripheral α2b-receptors at higher concentrations causes vasoconstriction, thereby offsetting the vasodilation from activation of the α2a-receptor (Ebert et al., 2000). In this respect, bradycardia is a prominent feature in clinical settings, while hypotension is relatively infrequent. Low incidence of hypotension may be due to the provision of sufficient preoperative hydration to the patients or the use of ephedrine for treatment. The use of a protocol that increases the time interval between dosage adjustments may reduce DEX-associated hypotension (Gerlach et al., 2009).

The method outlined in this paper is not without limitations. In particular, there is a risk that DEX may interact with other treatments or exacerbate existing pathologies. This may limit its applicability for imaging in some preclinical studies. However, the highly transient nature of the drug in the bloodstream may also reduce unexpected interactions.

Conclusion

We have demonstrated the use of dexmedetomidine for the reduction of involuntary tissue movement during intravital microscopy of the mouse liver using two-photon microscopy and have shown that it reduces fluorescence signal variation and increases image consistency. Dexmedetomidine is already FDA-approved and well-tolerated with similar effects in several different mammalian species, suggesting that the use of DEX for image stabilization can be easily generalized for use in a variety of preclinical animal models and clinical research.

Supplementary material. To view supplementary material for this article, please visit https://doi.org/10.1017/S1431927622000708

Financial support. This work was funded by the Basic Science Research Program (2019R1A2C2084122); by an MRC grant (2018R1A5A2020732) through the National Research Foundation of Korea (NRF); by the Ministry of Science & ICT (MSIT); the Ministry of Trade, Industry & Energy (MOTIE) under the Industrial Technology Innovation Program (20000843); Korea Health Technology R&D Project through the Korea Health Industry Development Institute (KHIDI), funded by the Ministry of Health & Welfare, Republic of Korea (HI18C2391). This study was supported by a grant (2022IP0053) from the Asan Institute for Life Sciences, Asan Medical Center, Seoul, Korea.

Conflict of interest. The authors declare that they have no competing interest.

References

Afonso J & Reis F (2012). Dexmedetomidine: Current role in anesthesia and intensive care. *Braz J Anesthesiol* **62**, 118–133.

Anderson GF & Fredericks CM (1977). Characterization of the oxybutynin antagonism of drug-induced spasms in detrusor. *Pharmacology* **15**, 31–39.

Belykh E, Miller EJ, Hu D, Martirosyan NL, Woolf EC, Scheck AC, Byvaltsev VA, Nakaji P, Nelson LY, Seibel EJ & Preul MC (2018). Scanning fiber endoscope improves detection of 5-aminolevulinic acid-induced protoporphyrin IX fluorescence at the boundary of infiltrative glioma. *World Neurosurg* **113**, e51–e69.

Bloor BC, Ward DS, Belleville JP & Maze M (1992). Effects of intravenous dexmedetomidine in humans. *Anesthesiology* **77**, 1134–1142.

Cai Y, Xu H, Yan J, Zhang L & Lu Y (2014). Molecular targets and mechanism of action of dexmedetomidine in treatment of ischemia/reperfusion injury (review). *Mol Med Rep* **9**, 1542–1550.

Choo YW, Jeong J & Jung K (2020). Recent advances in intravital microscopy for investigation of dynamic cellular behavior *in vivo*. *BMB Rep* **53**, 357–366.

Civantos Calzada B & Aleixandre de Artiñano A (2001). Alpha-adrenoceptor subtypes. *Pharmacol Res* **44**, 195–208.

Coste A, Oktay MH, Condeelis JS & Entenberg D (2020). Intravital imaging techniques for biomedical and clinical research. *Cytometry A* **97**, 448–457.

DeFily DV (1997). Fluorescence intravital microscopy of the coronary microvasculature. *Microsc Microanal* **3**, 321–322.

DeGroot WD, Tobias KM, Browning DC & Zhu X (2020). Examination of laryngeal function of healthy dogs by using sedation protocols with dexmedetomidine. *Vet Surg* **49**, 124–130.

Denk W, Strickler JH & Webb WW (1990). Two-photon laser scanning fluorescence microscopy. *Science* **248**, 73–76.

Ding L, Zhang H, Mi W, Wang T, He Y, Zhang X, Ma X & Li H (2015). Effects of dexmedetomidine on anesthesia recovery period and postoperative cognitive function of patients after robot-assisted laparoscopic radical cystectomy. *Int J Clin Exp Med* **8**, 11388–11395.

Dold C, Zaitsev M, Speck O, Firle EA, Hennig J & Sakas G (2006). Advantages and limitations of prospective head motion compensation for MRI using an optical motion tracking device. *Acad Radiol* **13**, 1093–1103.

Ebert TJ, Hall JE, Barney JA, Uhrich TD & Colinco MD (2000). The effects of increasing plasma concentrations of dexmedetomidine in humans. *Anesthesiology* **93**, 382–394.

Elbaradie S, El Mahalawy FH & Solyman AH (2004). Dexmedetomidine vs. Propofol for short-term sedation of postoperative mechanically ventilated patients. *J Egypt Natl Cancer Inst* **16**, 153–158.

Gerlach AT, Dasta JF, Steinberg S, Martin LC & Cook CH (2009). A new dosing protocol reduces dexmedetomidine-associated hypotension in critically ill surgical patients. *J Crit Care* **24**, 568–574.

Gertler R, Brown HC, Mitchell DH & Silvius EN (2001). Dexmedetomidine: A novel sedative-analgesic agent. *Bayl Univ Med Cent Proc* **14**, 13–21.

Giovannitti JA, Thoms SM & Crawford JJ (2015). Alpha-2 adrenergic receptor agonists: A review of current clinical applications. *Anesth Progress* **62**, 31–38.

Girard DS, Sutton JP, Williams TH, Crumbley AJ, Zellner JL, Kratz JM & Crawford FA (2004). Papaverine delivery to the internal mammary artery pedicle effectively treats spasm. *Ann Thorac Surg* **78**, 1295–1298.

Helmchen F & Denk W (2005). Deep tissue two-photon microscopy. *Nat Methods* **2**, 932–940.

Helmchen F & Denk W (2006). Erratum: Corrigendum: Deep tissue two-photon microscopy. *Nat Methods* **3**, 235–235.

Hong J-Y, Kim WO, Yoon Y, Choi Y, Kim S-H & Kil HK (2012). Effects of intravenous dexmedetomidine on low-dose bupivacaine spinal anaesthesia in elderly patients: Dexmedetomidine and spinal anaesthesia in elderly patients. *Acta Anaesthesiol Scand* **56**, 382–387.

Hughes CG, Mailloux PT, Devlin JW, Swan JT, Sanders RD, Anzueto A, Jackson JC, Hoskins AS, Pun BT, Orun OM, Raman R, Stollings JL, Kiehl AL, Duprey MS, Bui LN, O'Neal HR, Snyder A, Gropper MA, Guntupalli KK, Stashenko GJ, Patel MB, Brummel NE, Girard TD, Dittus RS, Bernard GR, Ely EW & Pandharipande PP (2021). Dexmedetomidine or propofol for sedation in mechanically ventilated adults with sepsis. *N Engl J Med* **384**, 1424–1436.

Ihler F, Bertlich M, Weiss B, Dietzel S & Canis M (2015). Two-photon microscopy allows imaging and characterization of cochlear microvasculature in vivo. *BioMed Res Int* **2015**, 1–8.

Jang M, Jung T, Kim S-H & Noh J (2019). Sex differential effect of dexmedetomidine on fear memory extinction and anxiety behavior in adolescent rats. *Neurosci Res* **149**, 29–37.

Karol MD & Maze M (2000). Pharmacokinetics and interaction pharmacodynamics of dexmedetomidine in humans. *Best Pract Res Clin Anaesthesiol* **14**, 261–269.

Kassell NF, Helm G, Simmons N, Phillips CD & Cail WS (1992). Treatment of cerebral vasospasm with intra-arterial papaverine. *J Neurosurg* **77**, 848–852.

Kim JK, Vinarsky V, Wain J, Zhao R, Jung K, Choi J, Lam A, Pardo-Saganta A, Breton S, Rajagopal J & Yun SH (2012). In vivo imaging of tracheal epithelial cells in mice during airway regeneration. *Am J Respir Cell Mol Biol* **47**, 864–868.

Koenig K, So PTC, Mantulin WW & Gratton E (1996). Cell damage in two-photon microscopes. Bigio IJ, Grundfest WS, Schneckenburger H, Svanberg K, & Viallet PM (Eds.), p. 172. Vienna, Austria. Available at http://proceedings.spiedigitallibrary.org/proceeding.aspx?doi=10.1117/12.260794 (accessed February 10, 2022).

Laffray S, Pagès S, Dufour H, De Koninck P, De Koninck Y & Côté D (2011). Adaptive movement compensation for In vivo imaging of fast cellular dynamics within a moving tissue. *PLoS One* **6**, e19928.

Lee S, Vinegoni C, Feruglio PF & Weissleder R (2012). Improved intravital microscopy via synchronization of respiration and holder stabilization. *J Biomed Opt* **17**, 0960181.

Lesur O, Chagnon F, Lebel R & Lepage M (2019). In vivo endomicroscopy of lung injury and repair in ARDS: Potential added value to current imaging. *J Clin Med* **8**, 1197.

Mason KP, Lubisch NB, Robinson F & Roskos R (2011). Intramuscular dexmedetomidine sedation for pediatric MRI and CT. *Am J Roentgenol* **197**, 720–725.

Matsuura R, Miyagawa S, Fukushima S, Goto T, Harada A, Shimozaki Y, Yamaki K, Sanami S, Kikuta J, Ishii M & Sawa Y (2018). Intravital imaging with two-photon microscopy reveals cellular dynamics in the ischeamia-reperfused rat heart. *Sci Rep* **8**, 15991.

Micieli F, Santangelo B, Reynaud F, Mirra A, Napoleone G, Della Valle G, Portier KG & Vesce G (2017). Sedative and cardiovascular effects of intranasal or intramuscular dexmedetomidine in healthy dogs. *Vet Anaesth Analg* **44**, 703–709.

Nelson LE, Lu J, Guo T, Saper CB, Franks NP & Maze M (2003). The α2-adrenoceptor agonist dexmedetomidine converges on an endogenous sleep-promoting pathway to exert Its sedative effects. *Anesthesiology* **98**, 428–436.

Noh C-K, Lim CS, Lee GH, Cho MK, Lee HW, Roh J, Kim YB, Lee E, Park B, Kim HM & Shin SJ (2021). A diagnostic method for gastric cancer using two-photon microscopy with enzyme-selective fluorescent probes: A pilot study. *Front Oncol* **11**, 634219.

Park I, Hong S, Hwang Y & Kim P (2020). A novel pancreatic imaging window for stabilized longitudinal *In vivo* observation of pancreatic islets in murine model. *Diabetes Metab J* **44**, 193.

Philipp M, Brede M & Hein L (2002). Physiological significance of α_{2}-adrenergic receptor subtype diversity: One receptor is not enough. *Am J Physiol-Regul, Integr Comp Physiol* **283**, R287–R295.

Pichol-Thievend C, Julien B, Anézo O, Philip B & Seano G (2021). Intravital imaging of brain tumors. In *Brain Tumors*. vol. **158**, Neuromethods, Seano, G. (Ed.), pp. 85–102. New York, NY: Springer US. Available at http://link.springer.com/10.1007/978-1-0716-0856-2_4 (accessed February 9, 2022).

Pilonis ND, Januszewicz W & Di Pietro M (2022). Confocal laser endomicroscopy in gastro-intestinal endoscopy: Technical aspects and clinical applications. *Transl Gastroenterol Hepatol* **7**, 7–7.

Pittet MJ & Weissleder R (2011). Intravital imaging. *Cell* **147**, 983–991.

Pnevmatikakis EA & Giovannucci A (2017). NoRMCorre: An online algorithm for piecewise rigid motion correction of calcium imaging data. *J Neurosci Methods* **291**, 83–94.

Shukry M & Miller JA (2010). Update on dexmedetomidine: Use in nonintubated patients requiring sedation for surgical procedures. *Ther Clin Risk Manag* **6**, 111–121.

Soulet D, Lamontagne-Proulx J, Aubé B & Davalos D (2020). Multiphoton intravital microscopy in small animals: Motion artefact challenges and technical solutions. *J Microsc* **278**, 3–17.

Vats R, Kaminski TW & Pradhan-Sundd T (2021). Intravital imaging of hepatic blood biliary barrier in live mice. *Curr Protoc* **1**, e256.

Venn RM, Bradshaw CJ, Spencer R, Brealey D, Caudwell E, Naughton C, Vedio A, Singer M, Feneck R, Treacher D, Willatts SM & Grounds RM (1999). Preliminary UK experience of dexmedetomidine, a novel agent for postoperative sedation in the intensive care unit. *Anaesthesia* **54**, 1136–1142.

Venn RM, Hell J & Michael Grounds R (2000). Respiratory effects of dexmedetomidine in the surgical patient requiring intensive care. *Crit Care* **4**, 302.

Vinegoni C, Lee S, Feruglio PF & Weissleder R (2014). Advanced motion compensation methods for intravital optical microscopy. *IEEE J Sel Top Quantum Electron* **20**, 83–91.

Woodward SC, Herrmann JB, Cameron JL, Brandes G, Pulaski J & Leonard F (1965). Histotoxicity of cyanoacrylate tissue adhesive in the Rat. *Ann Surg* **162**, 113–122.

Yin B, Piao Z, Nishimiya K, Hyun C, Gardecki JA, Mauskapf A, Jaffer FA & Tearney GJ (2019). 3D cellular-resolution imaging in arteries using few-mode interferometry. *Light Sci Appl* **8**, 104.

Yu S-B (2012). Dexmedetomidine sedation in ICU. *Korean J Anesthesiol* **62**, 405.

Zipfel WR, Williams RM & Webb WW (2003). Nonlinear magic: Multiphoton microscopy in the biosciences. *Nat Biotechnol* **21**, 1369–1377.

https://doi.org/10.1017/S1431927622000708 Published online by Cambridge University Press